

Fission yeast Swi5/Sfr1 and Rhp55/Rhp57 differentially regulate Rhp51-dependent recombination outcomes

Yufuko Akamatsu^{1,4}, Yasuhiro Tsutsui², Takashi Morishita^{1,5}, MD Shahjahan P Siddique¹, Yumiko Kurokawa¹, Mitsunori Ikeguchi¹, Fumiaki Yamao², Benoit Arcangioli³ and Hiroshi Iwasaki^{1,*}

¹International Graduate School of Arts and Sciences, Yokohama City University, Yokohama, Kanagawa, Japan, ²Division of Mutagenesis, National Institute of Genetics, Mishima, Shizuoka, Japan and ³Departement de la Structure et Dynamique des Genomes, Institut Pasteur, Paris Cedex 15, France

Several accessory proteins referred to as mediators are required for the full activity of the Rad51 (Rhp51 in fission yeast) recombinase. In this study, we analyzed *in vivo* functions of the recently discovered Swi5/Sfr1 complex from fission yeast. In normally growing cells, the Swi5-GFP protein localizes to the nucleus, where it forms a diffuse nuclear staining pattern with a few distinct foci. These spontaneous foci do not form in *swi2Δ* mutants. Upon UV irradiation, Swi5 focus formation is induced in *swi2Δ* mutants, a response that depends on Sfr1 function, and Sfr1 also forms foci that colocalize with damage-induced Rhp51 foci. The number of UV-induced Rhp51 foci is partially reduced in *swi5Δ* and *rhp57Δ* mutants and completely abolished in an *swi5Δ rhp57Δ* double mutant. An assay for products generated by HO endonuclease-induced DNA double-strand breaks (DSBs) reveals that Rhp51 and Rhp57, but not Swi5/Sfr1, are essential for crossover production. These results suggest that Swi5/Sfr1 functions as an Rhp51 mediator but processes DSBs in a manner different from that of the Rhp55/57 mediator.

The EMBO Journal (2007) 26, 1352–1362. doi:10.1038/sj.emboj.7601582; Published online 15 February 2007

Subject Categories: genome stability & dynamics

Keywords: crossover; DNA double-strand break repair; gene conversion; homologous recombination; Rad51 mediator

Introduction

The mechanism of homologous recombination (HR) has been studied extensively in *Saccharomyces cerevisiae* (reviewed in

*Corresponding author. Division of Molecular and Cellular Biology, International Graduate School of Arts and Sciences, Yokohama City University, 1-7-29 Suehiro-cho, Tsurumi-ku, Yokohama, Kanagawa 230-0045, Japan. Tel.: +81 45 508 7238; Fax: +81 45 508 7269; E-mail: iwasaki@tsurumi.yokohama-cu.ac.jp

⁴Present address: Developmental Biology Program, Memorial Sloan-Kettering Cancer Center, 1275 York Avenue, New York, NY 10021, USA

⁵Present address: Genome Damage and Stability Centre, University of Sussex, Brighton BN1 9RQ, UK

Received: 16 February 2006; accepted: 8 January 2007; published online: 15 February 2007

Paques and Haber, 1999; Symington, 2002; Krogh and Symington, 2004). Both meiotic and mitotic HR are initiated by DNA double-strand breaks (DSBs). The ends of DSBs are nucleolytically processed to form invasive 3' single-stranded DNA (ssDNA) tails, which are subsequently coated by replication protein A (RPA). Recombinase mediators such as Rad52 and the Rad55/Rad57 heterodimer assist Rad51-nucleoprotein filament formation by displacing RPA from ssDNA. The Rad51 filament searches for a homologous DNA duplex, with which it forms a D-loop or single-end invasion (SEI) intermediate. Rad51-mediated strand exchange has been shown to be enhanced by the Rad55/57 mediator *in vitro* (Sung, 1997). In the original DSB repair (DSBR) model (Szostak *et al.*, 1983), the annealed invading strand was proposed to be extended by DNA synthesis, resulting in the formation of a double Holliday junction (dHJ) intermediate. Resolution of the dHJ in one orientation was predicted to yield a crossover (CO) recombinant, whereas resolution in the other orientation results in a non-CO recombinant. However, recent studies suggest that dHJ intermediates formed during meiotic recombination are programmed to be resolved predominantly into COs and that non-CO recombinants are produced by an alternative pathway that does not involve Holliday junction intermediates (Allers and Lichten, 2001; Hunter and Kleckner, 2001). Non-COs have been proposed to arise by displacement of the extended invading strand in a D-loop, followed by reannealing to the 3'-tailed ssDNA on the other side of the break (Allers and Lichten, 2001; Hunter and Kleckner, 2001), in a pathway referred to as 'synthesis-dependent strand annealing' (SDSA) (Paques and Haber, 1999). Importantly, the decision between the meiotic CO and non-CO pathways is suggested to be made very early, before or during stable strand exchange (Allers and Lichten, 2001; Hunter and Kleckner, 2001; Börner *et al.*, 2004).

In contrast, mitotic cells from many organisms produce predominantly gene conversion without CO via the SDSA pathway and negatively regulate CO production that arises via dHJ formations (hereafter, we refer to gene conversion without CO as GC and to gene conversion with CO as CO). Because CO production may cause potentially deleterious chromosomal rearrangements, cells have evolved efficient systems to limit CO production. For instance, it has been suggested that the dissolution of dHJs by the combined action of RecQ family helicases and topoisomerase III leads to the suppression of COs in mitosis (Ira *et al.*, 2003; Wu and Hickson, 2003). However, it is still unclear how cells choose between the SDSA and DSBR pathways and which factors are specifically involved in mitotic dHJ formation.

Structural and functional homologues of *S. cerevisiae* recombination genes/proteins have been identified in many organisms, including the distantly related fission yeast *Schizosaccharomyces pombe*. The *S. pombe rad22⁺* is a homologue of *S. cerevisiae* RAD52 (Ostermann *et al.*, 1993),

and *rhp51⁺*, *rhp54⁺*, *rhp55⁺* and *rhp57⁺* (*rad* homologue of *S. pombe*) correspond to *S. cerevisiae* *RAD51*, *RAD54*, *RAD55* and *RAD57*, respectively (Muris *et al.*, 1993, 1996; Khasanov *et al.*, 1999; Tsutsui *et al.*, 2000). Additionally, two other genes, *swi5⁺* and *sfr1⁺*, have been implicated in HR and homologous recombinational repair (HRR) (Akamatsu *et al.*, 2003; Ellermeier *et al.*, 2004). The *swi5⁺* gene was first identified as one of the *swi* genes that are required for efficient mating-type (MT) switching in *S. pombe* (Egel *et al.*, 1984).

MT switching in *S. pombe* occurs efficiently during the mitotic cell cycle by GC of the transcriptionally active *mat1* locus using information from one of two silent cassettes (*mat2-P* and *mat3-M*). This GC-directed MT switching is assumed to arise through an SDSA-like process, which is initiated by a transient DSB associated with DNA replication (Arcangioli and de Lahondes, 2000; Dalgaard and Klar, 2001). Swi5, together Swi2 and Swi6, is implicated in promoting correct unidirectional GC (for review, see Klar, 1992; Arcangioli and Thon, 2004). The Swi6 protein is a homologue of the mammalian heterochromatin protein HP1, but the functions of Swi2 and Swi5 in MT remain unclear.

In a previous study, we showed that a protein complex containing Swi5 and Swi2 specifically promotes MT switching, whereas another complex containing Swi5 and Sfr1 is involved in Rhp51-dependent HRR (Akamatsu *et al.*, 2003). Sfr1 shares sequence homology with the C-terminal half of Swi2, the region that is important for Rhp51 and Swi5 binding, whereas Sfr1 lacks the Swi6-binding region. Epistasis analysis revealed that the Swi5/Sfr1 complex functions in a manner similar to, but independent of, the Rhp55/Rhp57 mediator. We recently showed that a stable Swi5/Sfr1 protein complex stimulates Rhp51-mediated DNA strand exchange *in vitro* (Haruta *et al.*, 2006).

Here, we present *in vivo* evidence that the Swi5/Sfr1 complex functions as a mediator that promotes and/or stabilizes Rhp51 filament formation. In addition, an assay for site-specific DSBR (Prudden *et al.*, 2003) indicated that canonical CO products were detected at low but significant frequencies in wild-type, *swi5Δ* and *sfr1Δ* strains, whereas they were not detected in *rhp57Δ* and *rhp51Δ* single mutant strains and in *rhp57Δ swi5Δ* double mutant strain. We discuss the functional differences between the Swi5/Sfr1 and Rhp55/Rhp57 mediators.

Results

Swi2- and Sfr1-dependent localization of Swi5 in the nucleus

To obtain further insight into the molecular functions of Swi5, EGFP was fused to the carboxyl terminus of Swi5 and its cellular localization was determined (Figure 1). The Swi5-EGFP fusion was fully functional as judged by MMS and UV sensitivity assays and by MT switching efficiency (data not shown). In normally growing cells, Swi5-EGFP localized to the nucleus and exhibited diffuse nuclear staining with a few distinct foci (Figure 1A). We previously reported that Swi5 genetically and physically interacts with the paralogues Swi2 and Sfr1 (Akamatsu *et al.*, 2003). We examined the effects of these gene functions on Swi5 localization in this study. In *swi2Δ* cells, Swi5-EGFP did not form nuclear foci, although it was still diffusely distributed in the nucleus. On the other hand, the nuclei of *sfr1Δ* cells contained Swi5-EGFP foci,

although the diffuse signal was almost undetectable. In *swi2Δ sfr1Δ* double mutant cells, Swi5-EGFP was not present in the nucleus, either in a diffuse pattern or in the form of foci. The absence of Swi2 or Sfr1 did not affect the cellular expression level of the Swi5-EGFP protein (Figure 1B). These results indicate that Swi2 and Sfr1 independently target Swi5 to the nucleus in normally growing cells: the former is required for distinct focus formation and the latter for diffuse nuclear distribution.

Swi5 and Swi2 associate on heterochromatin with Swi6

We next investigated the cellular localization of Swi2. The EGFP tag was fused to the amino terminus of endogenous Swi2 and the expressed fusion protein was fully functional, as judged by the efficiency of MT switching (data not shown). Although the EGFP-Swi2 signals were extremely weak, we could detect a few Swi2 nuclear foci, with a pattern very similar to that of Swi5-EGFP foci (Figure 1C). In contrast, we could not detect Swi2 foci in *swi5Δ* cells. The focal distributions of Swi2 and Swi5 were in turn very similar to that previously reported for Swi6 (Ekwall *et al.*, 1995). We therefore more closely examined whether spontaneous Swi5 and Swi2 foci colocalize with Swi6. As shown in Figure 1D and E, about 80% of Swi5-EGFP foci (93/117 total Swi5-EGFP foci) and 97% of EGFP-Swi2 foci (36/37 total EGFP-Swi2 foci) overlapped with Swi6-EGFP foci. The patterns of Swi6-EGFP in *swi5Δ* and *swi2Δ* mutants were very similar to those in wild-type cells (data not shown). In contrast, Swi2 foci were not detected in *swi6Δ* or *swi5Δ* mutant backgrounds (Figure 1C). This result is consistent with a previous demonstration of the colocalization of Swi6 and Swi2 at the *mat* locus by ChIP analysis by Jia *et al.* (2004). Although we could not detect the direct colocalization of Swi2 and Swi5 because both proteins were fused to the same tag, most Swi2 and Swi5 foci have been suggested to associate with Swi6. Interestingly, Swi5-EGFP foci formed in *swi6Δ* cells, although their intensities were drastically reduced (Figure 1A).

Sfr1 diffusely localizes in the nucleus in normally growing cells

We then examined the cellular localization of Sfr1. Endogenous EGFP-Sfr1 tagged at its amino terminus appeared to be functional, as judged by the MMS and UV sensitivities of cells with the fusion (data not shown). As shown in Figure 2A, EGFP-Sfr1 localized to the nucleus but did not form foci under normal growth conditions, like Swi5-EGFP in *swi2Δ* cells (Figure 1A). In the absence of Swi5, the EGFP-Sfr1 signals disappeared and the EGFP-Sfr1 protein could not be detected by immunoblot analysis (data not shown).

Rhp51-dependent assembly of the Swi5/Sfr1 foci upon UV irradiation

As both Sfr1 and Swi5 function in Rhp51-dependent HRR (Akamatsu *et al.*, 2003), we examined the distribution of Swi5-EGFP and EGFP-Sfr1 following UV irradiation. We previously showed that *swi2Δ* cells are fully proficient in UV repair (Akamatsu *et al.*, 2003), and as described above, they lack the spontaneous Swi5-EGFP foci that are normally present in heterochromatin (Figure 1A). Therefore, we used *swi2Δ* strains for analysis of induced Swi5 foci. More than 60% of *swi2Δ* cells formed Swi5 foci 3 h after UV irradiation,

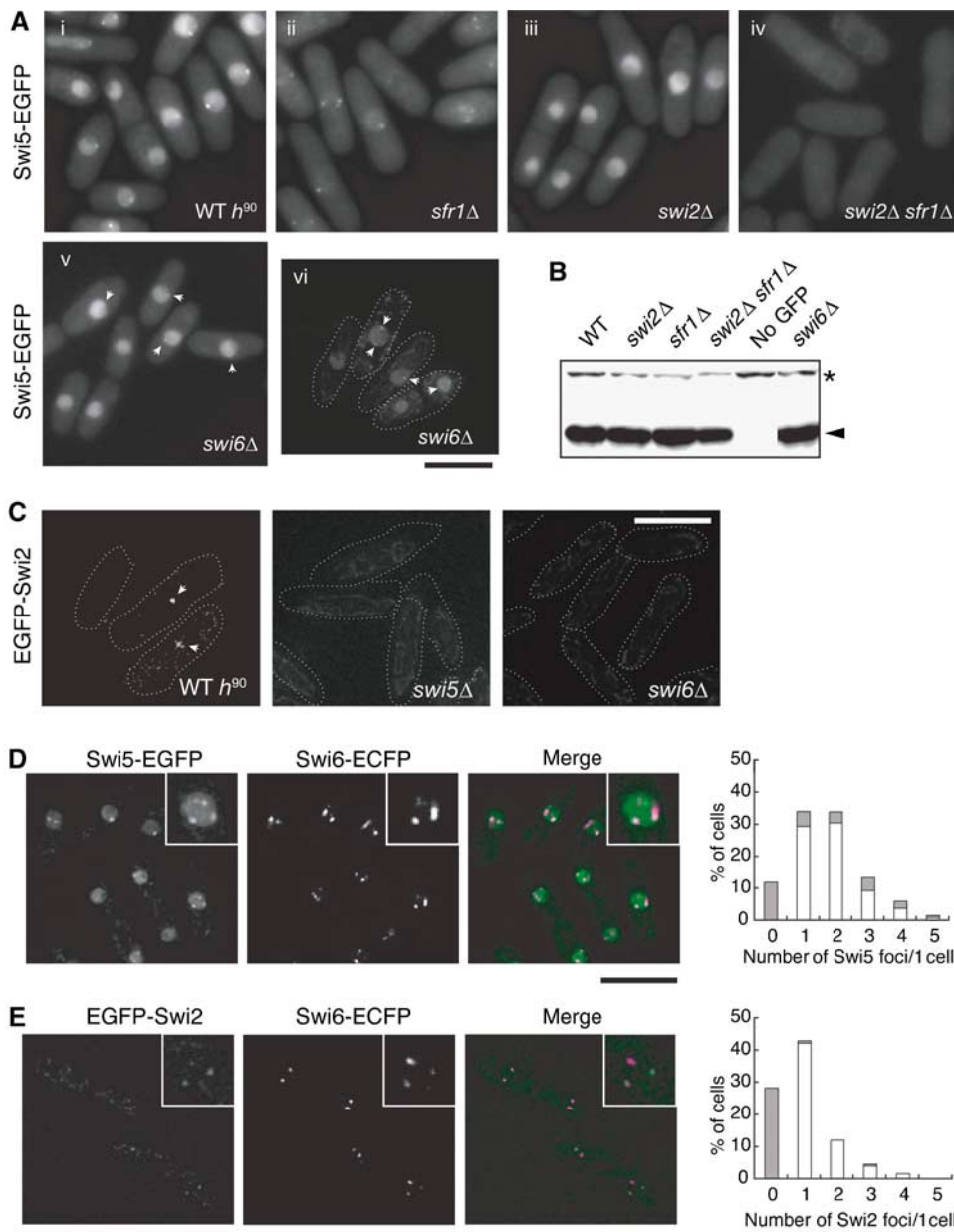


Figure 1 Localization of Swi2 and Swi5 proteins. (A) Swi5 localizes to the nucleus in two patterns. The diffuse nuclear localization of Swi5 is dependent on *sfr1*⁺, whereas focal formation requires *swi2*⁺. The Swi5-EGFP signals of exponentially growing cells were observed by fluorescence microscopy. The strains used were wild-type *h*⁹⁰ (YA598), *sfr1*Δ (YA763), *swi2*Δ (YA673), *swi2*Δ *sfr1*Δ (YA765) and *swi6*Δ (YA752). (i)–(v) Images were obtained by using a conventional fluorescence microscope (Nikon ECLIPSE E800). (vi) Image was obtained by using a DeltaVision microscope system as described in Materials and methods. The bar indicates 10 μm. (B) Neither the *swi2*Δ nor *sfr1*Δ mutation affects the level of Swi5-EGFP expression. Total protein extracts (10 μg) from the indicated strains were separated by SDS–polyacrylamide gel electrophoresis and subjected to immunoblot analysis with an anti-GFP antibody (JL-8, Clontech). The same strains were used as in (A) and the untagged strain was YA254. (C) Swi2 forms a few spontaneous foci in the nucleus. Swi2-EGFP signals of exponentially growing cells were observed by a DeltaVision microscope system. The strains used were wild type (YA820), *swi5*Δ (YA1247) and *swi6*Δ (YA1261). (D) Swi5 foci colocalize with Swi6 foci. A strain (YA756) with EGFP-tagged *swi5*⁺ and ECFP-tagged *swi6*⁺ was examined as in (C). In the merged image, green indicates Swi5-EGFP and magenta indicates Swi6-ECFP signals. Each inset is a magnified image of the same nucleus. The graph shows percentages of cells with unlocalized (gray bars) and colocalized (open bars) foci. X-axis gives the number of Swi5 foci in each cell. (E) Swi2 foci colocalize with Swi6 foci. A strain (YA1292) with EGFP-tagged *swi2*⁺ and ECFP-tagged *swi6*⁺ was examined as in (C). In the merged image, green indicates Swi2-EGFP and magenta indicates Swi6-ECFP signals. Each inset is a magnified image of the same nucleus. The graph shows percentages of cells with unlocalized (gray bars) and colocalized (open bars) foci. X-axis gives the number of Swi2 foci in each cell.

although the intensity of the foci was very weak (Figure 2B). Similarly, more than 60% of cells formed distinct EGFP-Sfr1 foci after UV irradiation (Figure 2B). The percentage of cells that formed Rhp51-ECFP was also a similar value under the same experimental condition (see below for the functionality and localization of Rhp51-ECFP protein). The intensity of

EGFP-Sfr1 foci was much stronger than that of induced Swi5-EGFP foci, which seemed to be weaker than the spontaneous foci formed in *swi2*⁺ cells. The UV-induced formation of Swi5-EGFP and EGFP-Sfr1 foci is completely dependent on Rhp51 function because Swi5-EGFP and EGFP-Sfr1 focal signals could not be detected in *rhp51*Δ mutants for up to

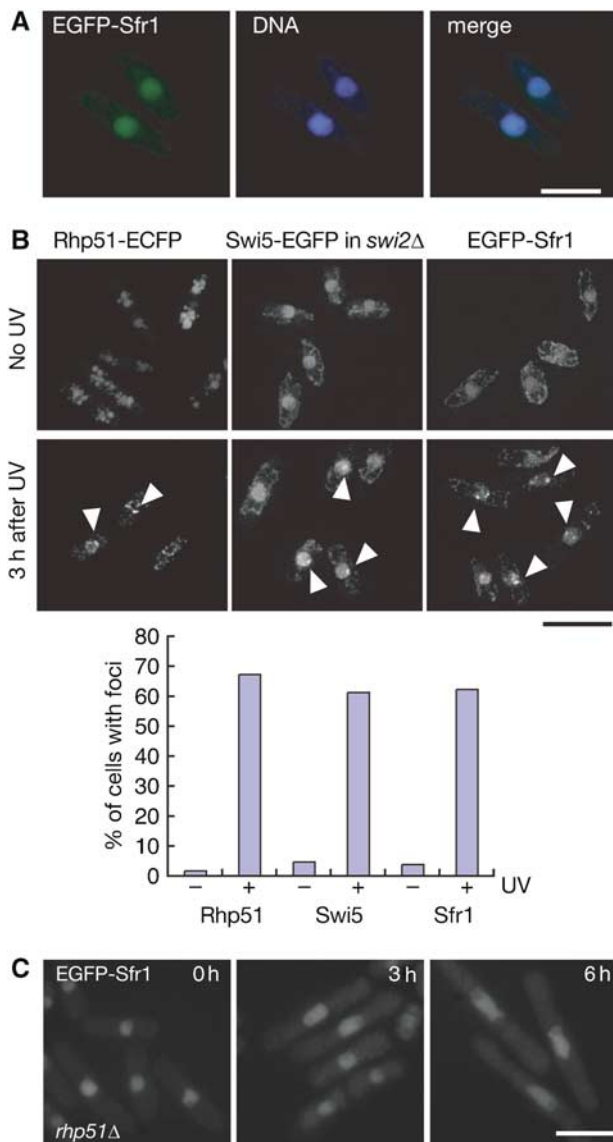


Figure 2 Analyses of damage-inducible Sfr1 and Swi5 foci. (A) The EGFP-Sfr1 signals and chromosomal DNA (stained with Hoechst 33342) of exponentially growing wild-type cells (YA848) were observed with a fluorescent microscope. (B) Rhp51 (left, YA990), Swi5 (middle, YA979) and Sfr1 (right, YA848) assemble following UV irradiation. Exponentially growing cells were irradiated with 100 J/m² UV light. After incubation for 3 h at 30°C, cells were observed by using a DeltaVision microscope system. Note that focal signals of Swi5-EGFP were analyzed in an *swi2Δ* background to abolish the accumulation of spontaneous foci at heterochromatin. The graph shows percentages of cells with foci before (–) and after (+) UV irradiation. (C) Sfr1 assembly is dependent on Rhp51. EGFP-Sfr1 focal signals are not detected in cells (YA986) with the *rhp51Δ* mutation 3 and 6 h after UV irradiation.

6 h after UV irradiation (Figure 2C and data not shown). Both the inducible Swi5 foci in the *swi2Δ sfr1Δ* strain and Sfr1 foci in the *swi5Δ* strain did not form upon UV irradiation (data not shown), indicating the mutual dependency of the inducible focus formation of the two proteins.

Accumulation and persistence of Swi5 and Sfr1 foci in *rhp54Δ* cells

Rhp54 and its budding yeast counterpart Rad54 are thought to function after Rhp51- and Rad51-mediated strand invasion, respectively (Muris *et al*, 1997; Symington, 2002). We then

examined Swi5 and Sfr1 focus formation in *rhp54Δ* cells (Figure 3A and B). A few weak EGFP-Sfr1 foci formed spontaneously in many *rhp54Δ* cells (about 60%) under normal culture conditions without UV irradiation (Figure 3A and B). UV irradiation enhanced the intensity of EGFP-Sfr1 foci more strongly in *rhp54Δ* cells than in wild-type cells. More than 90% of *rhp54Δ* cells exhibited EGFP-Sfr1 foci, compared with 60% of wild-type cells 3 h after UV irradiation. More than 80% of *rhp54Δ* cells exhibited Swi5-EGFP foci, compared with 60% of wild-type cells 3 h after UV irradiation under the same conditions. Swi5 and Sfr1 signals in *rhp54Δ* cells persisted longer than 26 h, whereas these signals disappeared gradually 8 h after UV irradiation in *rhp54+* cells. These observations suggest that Rhp54 is not required for Swi5 and Sfr1 focus formation *per se* but for their disassembly.

Association of Sfr1, Swi5 and Rhp51 at DNA damage sites

The induced Sfr1 and Swi5 foci described above most probably reflect DNA repair events mediated by HR. To obtain further evidence for this interpretation, we asked whether Rhp51 colocalizes with Swi5/Sfr1 upon induction of DNA damage. For this purpose, we fused ECFP to the carboxyl terminus of endogenous Rhp51. *rhp51-ECFP* cells exhibited UV sensitivity similar to that of *rhp51Δ* cells, and although the *rhp51-ECFP* gene did not complement the DNA repair defect of *rhp51Δ* cells, it did not affect the DNA repair activity of *rhp51+* cells (Supplementary Figure S1). These results indicate that *rhp51-ECFP* is a recessive allele of *rhp51+* with respect to DNA repair. However, the Rhp51-ECFP protein formed foci in the nucleus upon UV irradiation (Figure 2B). In addition, it formed a single focal signal in the nucleus when a DSB was induced in the Ch¹⁶-MG minichromosome (see below) as a result of HO endonuclease expression (Figure 4A). As no signal was observed in cells in which HO was not induced, the Rhp51-ECFP signal most likely represents the assembly of Rhp51 at the DSB site. Taking advantage of this property, we examined whether Rhp51 colocalizes with Swi5/Sfr1 upon induction of DNA damage (Figure 4B). Rhp51-ECFP formed several distinct nuclear foci upon UV irradiation and Swi5 and Sfr1 also formed limited numbers of foci. Almost all of the UV-induced EGFP-Sfr1 foci colocalized with Rhp51-ECFP foci (78.9%, *n* = 109). The faint Swi5-EGFP foci induced by UV irradiation also seemed to colocalize with Rhp51 foci (72.4%, *n* = 105). However, the intensity of these foci was very weak and there was some overlap of Rhp51 foci with background noise, suggesting that the number of Swi5-EGFP foci may be overestimated. However, the results nonetheless indicate that Sfr1, probably together with Swi5, is recruited to DNA damage sites of Rhp51 assembly, as purified Swi5 and Sfr1 proteins form a stable complex *in vitro* (Haruta *et al*, 2006).

Notably, the Swi2-dependent spontaneous formation of Swi5-EGFP foci was not affected by the *smt-0* (a *cis* mutation that prevents DSB formation at the *mat1* locus) or *rhp51Δ* mutations (Figure 4C), indicating that these spontaneous foci of Swi5 are not caused by DSBs that arise during MT switching.

Swi5 and Rhp57 independently facilitate Rhp51 assembly at damage sites

We previously showed that the DNA repair defects of the *swi5Δ* and *rhp57Δ* single mutants are partially suppressed by

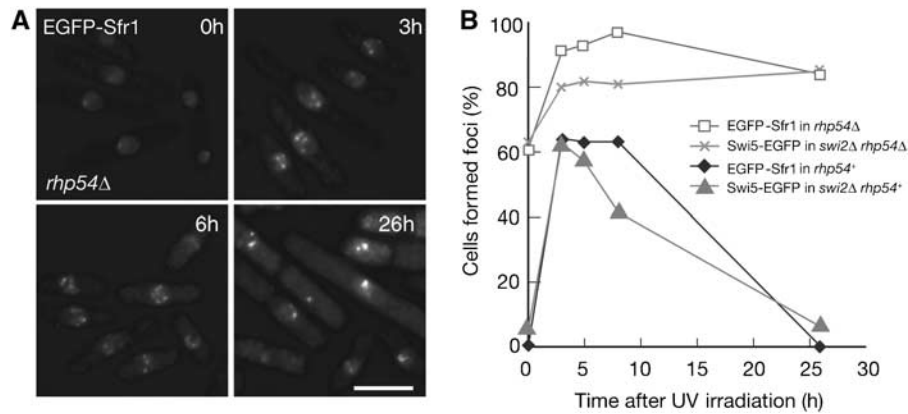


Figure 3 (A) In *rhp54Δ* cells (YA1240), EGFP-Sfr1 foci form spontaneously under normal growth conditions, but much more foci of stronger intensity are observed following UV irradiation (120 J/m^2). Foci persisted for at least 26 h after UV irradiation. (B) Time course of foci formations of Swi5 and Sfr1 after UV irradiation (120 J/m^2). Strains used were YA848 (EGFP-Sfr1), YA979 (Swi5-EGFP in *swi2Δ*), YA1325 (Swi5-EGFP in *swi2Δ rhp54Δ*) and YA1240 (EGFP-Sfr1 in *rhp54Δ*).

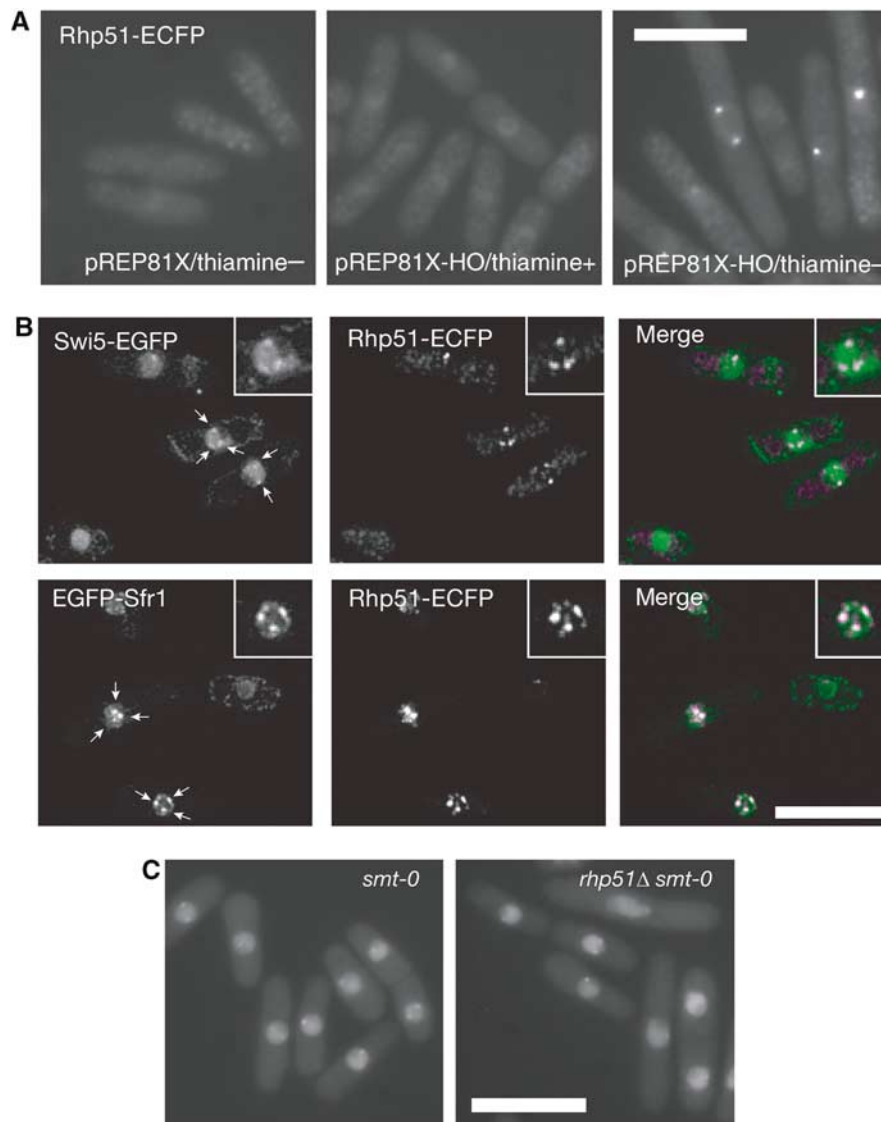


Figure 4 (A) Rhp51-ECFP assembles at sites of HO-induced single DSBs (YA1083). (B) Swi5 and Sfr1 colocalize with Rhp51 following UV irradiation. Top, cells with Swi5-EGFP and Rhp51-ECFP fusion proteins (YA1263); bottom, cells with EGFP-Sfr1 and Rhp51-ECFP fusion proteins (YA1213). Each inset is a magnified image of the same nucleus. In the merged images, green indicates Swi5-EGFP or EGFP-Sfr1 and magenta indicates Rhp51-ECFP signals. Each inset is a magnified image of the same nucleus. Note that focal signals of Swi5-EGFP were analyzed in a *swi2Δ* background to abolish the accumulation of spontaneous foci at heterochromatin. (C) Spontaneous Swi5 foci are independent of *rhp51+* and the DSB at the *smt* locus within the *mat1* region. The strains used were *rhp51+* *smt-0* (YA961) and *rhp51Δ* *smt-0* (YA984).

overexpression of *rhp51*⁺ (Tsutsui *et al*, 2000; Akamatsu *et al*, 2003). Here, we demonstrated that the UV sensitivity of the *swi5Δ rhp57Δ* double mutant was still partially suppressed by overexpression of *rhp51*⁺, indicating that the repair defects of these cells can be bypassed by a high concentration of Rhp51 (Figure 5A). The MMS sensitivity of the double mutant was also suppressed by *rhp51*⁺ overexpression (data not shown). These observations, together

with previous results, suggest that Swi5/Sfr1, like Rhp55/57 but independently of it, acts directly on the Rhp51 nucleoprotein filament. To explore this possibility, we examined the assembly of Rhp51 in UV-irradiated cells by immunostaining (Figure 5B and C). Wild-type cells formed nuclear foci upon UV irradiation. Very few signals were detected in unirradiated wild-type cells, and signals were not detected in irradiated *rhp51Δ* cells, indicating that the observed foci likely represent Rhp51 filaments assembled at DNA damage sites. More than 80% of wild-type nuclei exhibited significant signals, with about half (46%) of the nuclei having very strong signals. In *swi5Δ* cells, the percentage of nuclei with intense foci was strongly reduced to 6%, although the frequency of cells with weaker signals significantly increased (ca 30% in wild-type cells versus ca 60% in *swi5Δ* cells). Cells with the *rhp57Δ* mutation also showed a reduction in Rhp51 assembly: there were only half as many strong foci and there was a slight increase of weak foci, as compared with wild-type cells. These effects appeared to be less pronounced than in *swi5Δ* cells. The *swi5Δ rhp57Δ* double mutant was more severely affected than either single mutant. In particular, they had only a few nuclei with strong Rhp51 foci, and the frequency of cells with weak foci was much lower than that for the *rhp57Δ* and *swi5Δ* single mutants. The peak time of Rhp51 assembly after UV irradiation was not detectably affected by the *swi5Δ*, *rhp57Δ* or *swi5Δ rhp57Δ* mutations (data not shown). These results suggest that Swi5 and Rhp57 facilitate or stabilize Rhp51 nucleoprotein filament formation in a redundant manner. As the *S. cerevisiae* Rad55/57 heterodimer acts as a mediator that promotes Rad51-dependent strand exchange (Sung, 1997), the Swi5/Sfr1 complex likely functions as another Rhp51 mediator *in vivo*. Indeed, we have recently reported that the Swi5/Sfr1 complex stimulates *in vitro* strand exchange mediated by Rhp51 (Haruta *et al*, 2006).

Genetic assay of site-specific DSBR

To examine functional differences between the Swi5/Sfr1 and Rhp55/Rhp57 mediator complexes, we adopted the site-specific DSBR assay system established by Prudden *et al* (2003). In this system, a single DSB is created by the HO endonuclease at a 112-bp target site embedded in a non-essential minichromosome, Ch¹⁶-MG. A *kanMX* marker conferring G418 resistance is adjacent to the cut site. The presence of *ade6-M216* on Ch¹⁶-MG and *ade6-M210* on chromosome III confers an *ade*⁺ phenotype through intragenic complementation. An HO-induced DSB can be repaired by the NHEJ pathway or by HRR involving Ch¹⁶-MG and chromosome III. Failure to repair the DSB results in minichromosome loss,

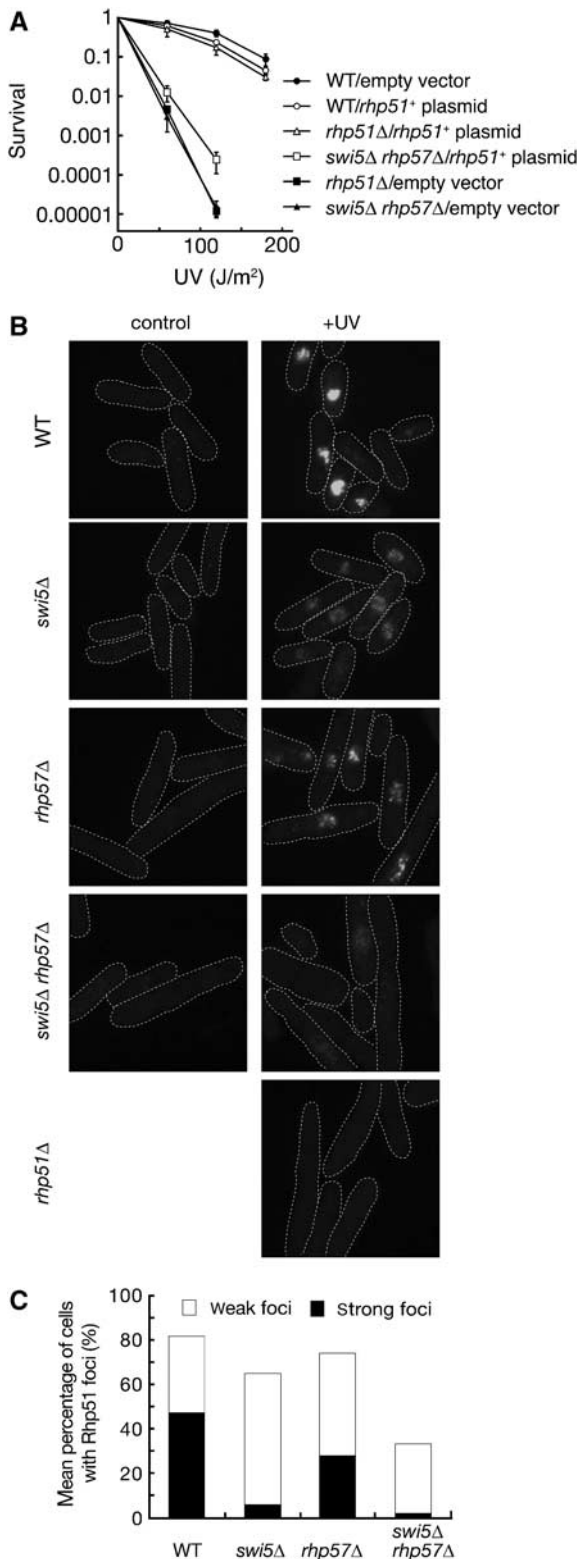


Figure 5 Rhp57- and Swi5-dependent subnuclear accumulation of Rhp51 upon UV irradiation. (A) A multicopy plasmid expressing *rhp51*⁺ suppresses the UV sensitivity of the *swi5Δ rhp57Δ* double mutant. Wild-type (YA119), *rhp51Δ* (T3) and *swi5Δ rhp57Δ* (YA250) cells carrying the vector alone (pSP102) or a vector expressing *rhp51*⁺ (pSP192) were examined for UV sensitivity. The data represent the average of the results from three independent experiments and standard deviations are shown by error bars. (B) Rhp51 accumulation in wild-type and mutant cells was detected by immunostaining with the anti-Rhp51 antibody. Wild-type (YA119), *swi5Δ* (YA177), *rhp57Δ* (T5), *swi5Δ rhp57Δ* (YA250) and *rhp51Δ* (T3) cells were examined without UV irradiation or 3 h after UV irradiation (200 J/m²). (C) Mean percentage of mutant cells showing Rhp51 foci at 3 h post-irradiation. Frequencies were determined as described in Materials and methods.

leading to an *ade*⁻ G418^s phenotype (see Supplementary Figure S2). Importantly, the single DSB is very efficiently generated within 48 h after induction, with no loss of cell viability (Prudden *et al*, 2003). Therefore, this system allows us to score most genetic events resulting in DSBR or failure to repair. The results of this genetic assay are shown in Supplementary Table S1. *ade*⁺ G418^s and *ade*⁻ G418^s segregants were efficiently produced upon HO induction, whereas there was no increase in the frequency of these colonies without induction, consistent with previous observations (Prudden *et al*, 2003).

Mediator mutations reduce HRR capacity for a single DSB

HRR-mediated *ade*⁺ G418^s segregants are expected to arise by GC and CO, whereas *ade*⁻ G418^s segregants are expected to arise mainly by minichromosome loss and long-tract gene conversion (LTGC) (Prudden *et al*, 2003). To quantify the proportion of each product, we prepared genomic DNA from independent colonies in each assay and determined the sizes of Ch¹⁶-MG and Chromosome III by pulse-field gel electrophoresis (PFGE). Among the *ade*⁺ G418^s segregants, we found three types of chromosomal patterns, as expected: one consisting of 0.5 and 3.5 Mb chromosomal bands that could be generated by canonical GC, one with two 2 Mb bands generated by canonical CO and one with 2 and 3.5 Mb bands that may be generated by non-reciprocal exchange associated with break-induced replication (referred to as BIR type 1). Among the *ade*⁻ G418^s segregants, we found four types of chromosomal patterns, as expected: one with only the 3.5 Mb chromosome band that could have resulted from failure to repair the DSB (Ch¹⁶-MG loss), one with 0.5

and 3.5 Mb bands generated by LTGC, one with two 2 Mb bands generated by a two-marker GC event associated with CO and one with 2 and 3.5 Mb bands generated by non-reciprocal exchange (referred to as BIR type 2) (see Supplementary Figures S2 and S3). To confirm that *ade6-M216* of Ch¹⁶-MG is indeed converted to *ade6-M210* in the segregants that we classified as LTGC, we analyzed the DNA sequences of the *ade6* gene of *ade*⁻ G418^s segregants with 0.5 and 3.5 Mb bands, which were obtained very frequently from *rhp57Δ* (see the next section). All *ade*⁻ G418^s segregants with 0.5 and 3.5 Mb bands had a homologous *ade6-M210* sequence, indicating that they were generated by LTGC (Supplementary Figure S4). PFGE data are summarized in Supplementary Tables S2 and S3, and the ratios of HRR, NHEJ and Ch¹⁶-MG loss that were calculated using the results in Supplementary Tables S1–S3 are presented in Table I.

In the wild-type strain, the major outcome of DSB induction is HRR (73.3%), followed by minichromosome loss (16.2%) and NHEJ (10.5%). In the absence of Rhp51, the survivors produced by HRR were severely reduced in number and the frequency of minichromosome loss was dramatically elevated. These results agree very well with those previously reported (Prudden *et al*, 2003). The *rhp57Δ*, *swi5Δ* and *sfr1Δ* single mutations affected HRR more mildly than did the *rhp51Δ* mutation, although each slightly enhanced the frequency of NHEJ. The *swi5Δ rhp57Δ* double mutant showed a repair profile very similar to that of the *rhp51Δ* single mutant. All of these features are highly consistent with the UV and γ -ray sensitivities of this mutant that we previously reported (Akamatsu *et al*, 2003).

Mutations in recombination genes differentially affect the outcome of HRR

Table II shows the frequencies of different HRR outcomes among the total survivors. The wild-type strain repaired the single DSB mainly by GC (57% of total segregants, which corresponds to 78% of the HRR outcomes). Canonical CO and LTGC also occurred at much lower frequencies (6.3 and 7.4%, respectively). Others, including BIR types 1 and 2 and two-marker GC with CO and unknown products, appeared at low frequencies (2.6% in total). The frequencies of these minor recombinants are not statistically significant for the mutants tested in this study. The *rhp51Δ* mutation reduced GC (5.0%), abolished CO (not detected among 105 *ade*⁺ G418^s segregants analyzed by PFGE) and moderately increased LTGC (13.2%). These results, together with the increase in minichromosome loss (see above), underscore the central role of Rhp51 in HRR processes and indicate that an

Table I Summary of the outcomes (%) of single DSB induction

Strain	NHEJ	HRR	Minichromosome loss
Wild type (TH805)	10.5±2.1	73.3±2.4	16.2±0.7
<i>rhp51Δ</i> (TH895)	16.7±0.6	19.8±1.8	63.5±2.0
<i>rhp57Δ</i> (YA1095)	19.8±3.3	37.4±4.4	42.8±4.5
<i>swi5Δ</i> (YA1056)	33.1±2.6	36.4±2.3	30.5±2.0
<i>sfr1Δ</i> (YA1316)	25.5±3.4	43.0±2.4	31.5±2.6
<i>swi5Δ rhp57Δ</i> (YA1096)	24.8±4.5	17.6±3.4	57.5±4.6

Colonies that arose after HO induction were classified into three categories, NHEJ, HRR and minichromosome loss, by phenotypic and PFGE analyses. The average frequencies (total segregants = 100%) and standard errors were statistically determined by the bootstrap method (100 000 iterations) with the data sets in Supplementary Tables 1–3.

Table II Outcomes (%) of HRR among total survivors

Strain	GC	CO ^a	LTGC	BIR type 1	BIR type 2	Two-marker GC with CO	Unknown
Wild type (TH805)	57.0±2.7	6.3±1.1	7.4±0.6	1.0±0.9	1.4±0.3	0.2±0.2	No ^b
<i>Rhp51Δ</i> (TH895)	5.0±0.6	No ^b	13.2±1.1	No ^b	0.8±0.7	0.8±0.7	No ^b
<i>Rhp57Δ</i> (YA1095)	9.6±0.8	No ^b	27.0±3.9	No ^b	No ^b	0.6±0.5	0.3±0.1
<i>swi5Δ</i> (YA1056)	21.8±1.4	1.9±0.6	12.1±1.6	0.2±0.2	0.4±0.4	No ^b	No ^b
<i>sfr1Δ</i> (YA1316)	26.6±1.7	1.4±0.5	14.2±1.8	No ^b	0.8±0.7	No ^b	No ^b
<i>swi5Δ rhp57Δ</i> (YA1096)	2.7±0.5	No ^b	14.2±3.4	No ^b	No ^b	0.8±0.7	No ^b

The average frequencies of colonies produced by HRR (total HO-induced segregants = 100%) and standard errors were statistically determined by the bootstrap method (100 000 iterations) with the data sets of Supplementary Tables 1–3.

^aP-values determined by Fisher's exact test are presented in Supplementary Table S4.

^bNo colonies were obtained.

LTGC process is enabled or activated in the absence of Rhp51 function. Both the *swi5* Δ and *sfr1* Δ single mutations conferred very similar effects: they caused a much milder reduction in GC (21.8 and 26.6%, respectively) than did the *rhp51* Δ mutation and increased LTGC (12.1 and 14.2%, respectively) to a similar level.

The *rhp57* Δ mutation reduced GC to 9.6%, which was an effect milder than that of the *rhp51* Δ mutation but more severe than those of the *swi5* Δ and *sfr1* Δ mutations. Interestingly, the *rhp57* Δ mutation increased the frequency of LTGC (27.0%) more than did the *rhp51* Δ , *swi5* Δ or *sfr1* Δ mutations. The *swi5* Δ *rhp57* Δ double mutant produced each recombinant class at frequencies similar to that of the *rhp51* Δ single mutant, consistent with the idea that the double mutation completely abolishes the Rhp51-dependent repair pathway. The increased frequency of LTGC in the *rhp57* Δ single mutant was suppressed in the *swi5* Δ *rhp57* Δ double mutant (14.2%), a level similar to that observed in the *rhp51* Δ mutant, suggesting that the hyper-increase of LTGC in the *rhp57* Δ single mutant is produced by Rhp51 and Swi5 functions (probably together with Sfr1).

Most interestingly, *rhp51* Δ or *rhp57* Δ mutants yielded no CO segregants, whereas *swi5* Δ and *sfr1* Δ single mutants produced CO segregants at reduced levels relative to wild-type cells. Although the frequency of CO was low, these values are statistically significant (Supplementary Table S4). Therefore, these results clearly indicate the essential functions of Rhp51 and Rhp57 in CO production. The strong increases in LTGC and their essential role in CO production observed in this study are the first demonstration of a functional difference among HRR mediators.

Discussion

Localization of two Swi5-containing complexes

The study described here has shown two nuclear patterns for Swi5 (Figure 1). Swi5 (Swi2-dependent) and Swi2 foci overlap with some Swi6 foci. In fission yeast, the chromodomain protein Swi6 localizes to the silent *mat* loci, centromeres and telomeres. It has been demonstrated that Swi2 and Swi5, as well as Swi2 and Swi6, interact physically, allowing the chromodomain protein Swi6 of the Swi2/Swi5 mediator complex to spread into the silent *mat* region (Akamatsu *et al*, 2003; Jia *et al*, 2004). Taken together, these results suggest that the overlapping foci shown in Figure 1 localize to the MT region. The Swi2-independent subnuclear localization of Swi5 is required for the function of Sfr1, which also localizes in a diffuse manner to the subnuclear region under normal growing conditions (Figure 1). In turn, upon DNA-damaging treatment, Sfr1 and Swi5 foci are induced most probably at DNA damage sites where Rhp51 also forms foci (Figure 4). The induced formation of Swi5 foci does not require Swi2, which is also consistent with the fact that Swi2 is not required for DNA repair (Akamatsu *et al*, 2003). On the other hand, the inducible focus formation of Sfr1 and Swi5 is interdependent (Figure 1 and data not shown). In addition, their focus formations require Rhp51 (Figure 2C and data not shown). Thus, Rhp51, Swi5 and Sfr1 are mutually interdependent for association at DNA damage sites. Although we did not directly observe colocalization in this study because of technical difficulties related to tagging, this interdependency suggests that Swi5 and Sfr1 form a stable complex

in vivo. We previously reported physical interactions between Swi5 and Sfr1 *in vivo* (Akamatsu *et al*, 2003). Very recently, we have demonstrated that Swi5 and Sfr1 form a stable complex in solution, and that the Swi5/Sfr1 complex interacts with Rhp51 in an Sfr1-dependent manner (Haruta *et al*, 2006). Therefore, we conclude that the observed DNA damage-inducible Swi5 and Sfr1 foci contain a tight complex of the two proteins, and that these foci represent sites in which Rhp51-dependent HRR events occur.

The Swi5/Sfr1 complex is a novel mediator of Rhp51

We recently demonstrated that the Swi5/Sfr1 complex stimulates Rhp51-mediated strand exchange *in vitro* (Haruta *et al*, 2006). The results presented in this study provide several lines of further *in vivo* evidence that the Swi5/Sfr1 complex acts as a mediator for Rhp51. First, Swi5/Sfr1 foci are formed upon DNA damage and persist for a long period in the *rhp54* Δ mutant (Figure 3). Rad54 and its paralogues are thought to function after Rad51-mediated strand invasion (Muris *et al*, 1997; Symington, 2002). The observation of Swi5/Sfr1 foci in the *rhp54* Δ mutant suggests a defect in the disassembly of Rhp51 in this background, also implying that recombination reactions arrest and that toxic recombination intermediates accumulate in *rhp54* Δ cells. Consistent with this, it has been shown that both *S. pombe* Rhp51 in the *rhp54* Δ background and *S. cerevisiae* Rad51 in the *rad54* Δ background assemble at damage sites and that recombination does not progress further (Caspari *et al*, 2002; Sugawara *et al*, 2003; Miyazaki *et al*, 2004). Taken together, these data suggest that Swi5/Sfr1 functions upstream of Rhp54, probably with Rhp51.

Second, cytological analyses show that DNA damage-inducible Swi5/Sfr1 foci accumulate at sites of damage, where Rhp51 also forms foci (Figure 4). It was not possible in this study for technical reasons to demonstrate that Swi5, Sfr1 and Rhp51 simultaneously colocalize. However, inducible focus formation requires Rhp51 (Figure 2C) and normal levels of Rhp51 focus formation require Swi5 (Figure 5). The *swi5* Δ *rhp57* Δ double mutation abolishes Rhp51 focus formation (Figure 5). These findings suggest that the Swi5/Sfr1 complex and Rhp51 associate *in vivo* and that each factor is required for the full inducible accumulation at DNA damage sites.

Third, Rhp51 overproduction suppresses mutations affecting mediator functions. The partial suppression of the DNA repair defects of the *S. cerevisiae* *rad55* and *rad57* mutants by Rad51 overexpression can be interpreted as indicating that high concentrations of Rad51 are required for functional nucleoprotein filament formation in these mutants (for review, see Symington, 2002). The repair defects of the *swi5* Δ and *sfr1* Δ mutants are also suppressed by Rhp51 overexpression (Akamatsu *et al*, 2003), as is also the case for the *rhp55* Δ and *rhp57* Δ mutants (Muris *et al*, 1996; Khasanov *et al*, 1999; Tsutsui *et al*, 2000). Most importantly, the defects of the *swi5* Δ *rhp57* Δ and *sfr1* Δ *rhp57* Δ double mutants are also suppressed by Rhp51 overproduction (Figure 5A; Y Akamatsu and H Iwasaki, unpublished).

The Swi2/Swi5 complex may also play a mediator role in Rhp51-mediated strand exchange during MT switching, which is caused by a unidirectional GC most likely arising through an SDSA-like process (Klar, 1992; Arcangioli and Thon, 2004). As Swi5/Sfr1 is involved in the GC-producing pathway (see below), the two Swi5-containing complexes

may have similar intrinsic biochemical activities. A major difference is conferred by the Swi6 interaction, which stabilizes Swi2/Swi5 at the silent donor MT loci. Interestingly, spontaneous Swi5 foci are observed in *smt-0* strains regardless of Rhp51 function (Figure 4C). This implies that Swi2/Swi5 remain at the *mat* locus independently of the initiation of the MT switching reaction (Figure 4C).

Rhp51 and its mediator functions in DSBR

The single DSBR analysis described here has provided important information about DSBR pathways in *S. pombe* (Table II). First, canonical GC (gene conversion without CO) was reduced in the mutants tested in this study, indicating that Rhp51 and both the Rhp55/57 and Swi5/Sfr1 mediators are involved in GC production. Second, LTGC products were increased in all mutants, indicating that an Rhp51-independent pathway is responsible for the elevated level of LTGC. This pathway may involve Rad22 (Doe *et al*, 2004). Third, the *rhp57Δ* mutation generated more LTGC segregants than did the *rhp51Δ* mutation, but the *swi5Δ* mutation restored this frequency to that of the *rhp51Δ* single mutant. This suggests that the hyper-increase of LTGC in the *rhp57Δ* single mutant is produced by the functions of Rhp51 and the Swi5/Sfr1 mediator. Fourth, and most importantly, cells with the *rhp57Δ* or *rhp51Δ* mutation do not produce canonical CO products, whereas wild-type, *swi5Δ* and *sfr1Δ* strains produce low but significant levels of COs. The *rhp57Δ* mutation is epistatic to the *swi5Δ* mutation with respect to CO production. These results clearly indicate that Rhp51 and Rhp57 are required for CO production and that Rhp51 and its mediators play a critical role in GC/CO production during HRR. This conclusion is consistent with a report that a mammalian mediator complex containing Rad51C and XRCC3, a probable counterpart of Rhp55/Rhp57 (Tsutsui *et al*, 2000), is associated with branch migration and Holliday junction resolution activities *in vitro* (Liu *et al*, 2004). Furthermore, XRCC3 mutant cells have been reported to display drastically altered spectra of recombination products, with increased GC tract lengths, increased frequencies of discontinuous tracts and frequent local rearrangements associated with HR (Brenneman *et al*, 2002). Taken together, these results support the notion that mediator functions have been conserved through evolution.

A working hypothesis

In an attempt to interpret the data, we propose the following model for mitotic HRR (see also Supplementary Figure S5). Two major homology-dependent DSBR pathways, SDSA and DSBR, have been described (Paques and Haber, 1999). To avoid confusion with our conventional usage of DSBR for 'DNA DSBR', we hereafter refer to the model proposed by Szostak *et al* (1983) as sDSBR. SDSA produces only GC, whereas sDSBR can potentially produce both GC and CO via the formation and resolution of dHJs. In both pathways, the invasion of a single-strand 3'-tail into a homologous DNA duplex is the initial critical step (SEI or D-loop formation) and is mediated by Rhp51. In our model, mediators (Rhp55/57, Swi5/Sfr1 and Swi5/Swi2) are independently involved in this step. The Rhp51/55/57-mediated SEI intermediate can be resolved by either the sDSBR or SDSA pathways. The latter pathway produces only GCs. In sDSBR, the second Holliday junction is formed by the action of Rhp51/55/57, leading to

the formation of a dHJ. The resolution of dHJs can produce COs, as well as GCs, which are followed by the steps originally proposed by Szostak *et al* (1983). Rhp51/Swi5/Sfr1-mediated SEI is also resolved by the sDSBR or SDSA pathway. The Swi5/Sfr1 complex is not essential for CO production, but it is needed for wild-type levels of COs (Table II). Therefore, we assume that in the Swi5/Sfr1-dependent sDSBR pathway, the second Holliday junction is also formed by Rhp51/55/57 but not Rhp51/Swi5/Sfr1 functions. The resolution of dHJs leads to CO/GC production. In the case of MT switching, the Swi5/Swi2 complex, together with Swi6, might participate in the initiation and resolution steps, avoiding Rhp55/57 mediator recruitment and thereby favoring an SDSA-like process.

This simple model, although not the only possible model, accounts for many properties of the mutants in this study. For example, in *swi5Δ* or *sfr1Δ* mutants, Rhp55/57-mediated SEI is functional and can be resolved by either the sDSBR or SDSA pathways, leading to a reduced level of GC/CO production. In the *rhp57Δ* mutant, Rhp57-dependent SEI does not occur and the sDSBR pathway initiated by Rhp51/Swi5/Sfr1-mediated SEI is 'aborted', leading to the production of GC only through the SDSA pathway. The aborted intermediates in this sDSBR pathway may undergo continued extension of the invading ssDNA, resulting in a strong increase in LTGC. Although further studies will verify and improve this model, the results presented here clearly indicate that Rhp51 mediators are critically important factors for CO/GC production.

Meiotic functions of the Swi5/Sfr1 complex

The Sae3/Mei5 complex has been identified as a new assembly factor for the meiotic-specific Dmc1 recombinase in *S. cerevisiae* (Hayase *et al*, 2004; Tsubouchi and Roeder, 2004). Sae3 and Mei5 are apparent homologs of Swi5 and Sfr1, respectively, although *sae3* and *mei5* mutants do not exhibit mitotic DNA repair defects (McKee and Kleckner, 1997; Hayase *et al*, 2004). Both *swi5Δ* and *sfr1Δ* mutants were shown to have defects in meiosis (Ellermeier *et al*, 2004) (our unpublished data). We recently demonstrated that the Swi5/Sfr1 complex interacts directly with Dmc1 *in vitro* and stimulates strand exchange mediated by Dmc1 as well as by Rhp51 (Haruta *et al*, 2006). This finding indicates that Swi5/Sfr1 also acts as a Dmc1 mediator. However, as *S. pombe dmc1Δ* and *swi5Δ* mutants and *S. cerevisiae dmc1Δ*, *sae3Δ* and *mei5Δ* mutants are defective in CO production during meiosis (Bishop *et al*, 1992; Ellermeier *et al*, 2004; Tsubouchi and Roeder, 2004), the function of Swi5/Sfr1 in mitotic HRR seems to be different from that in the meiotic recombination. One way to resolve the disparity between the roles of Swi5/Sfr1 in mitotic HRR and meiotic recombination is to identify the mechanism by which cells choose between the Rhp51/Swi5/Sfr1 and Dmc1/Swi5/Sfr1 complexes. Alternatively, it is possible that Swi5/Sfr1 complex plays a role in coordinating the activities of Rhp51 and Dmc1.

Materials and methods

Strains, media and growth conditions

The *S. pombe* strains used in this study are shown in Supplementary Table S5. Strain constructions are also described in Supplementary data. Standard procedures were used for culture and genetic manipulations (Moreno *et al*, 1991).

Fluorescent tagging of the *Swi5*, *Sfr1*, *Swi2*, *Swi6* and *Rhp51* proteins

Details of procedures for fluorescent tagging are provided in Supplementary data.

Immunofluorescence analysis of damage-induced *Rhp51* foci

Exponentially growing cells were irradiated with UV light (200 J/m²). Following incubation for 3 h, cells were collected and immunostained as previously described (Hagan and Hyams, 1988). Rabbit anti-Rhp51 antibody (Akamatsu et al, 2003) was used as a primary antibody at a dilution of 1:2000, and Alexa Fluor 488-conjugated anti-rabbit antibody (Molecular Probes) was used as a secondary antibody at a dilution of 1:500. The signal intensity of each strain was determined with Lumina Vision (Mitani Corp., Japan), a fluorescence image analyzer. Arbitrary intensity units (0–255) were defined by the analyzer. Cells with intensity units of 100 or more were defined as ‘strong’ and those with 30–99 units were defined as ‘weak’.

Fluorescence microscopy

Exponentially growing cells were photographed using a Nikon Eclipse E800 microscope with a VFM epifluorescence attachment or a DeltaVision microscope system (Applied Precision Inc., Issaquah, WA) attached to an Olympus IX-70 fluorescence microscope.

References

- Akamatsu Y, Dziadkowiec D, Ikeguchi M, Shinagawa H, Iwasaki H (2003) Two different *Swi5*-containing protein complexes are involved in mating-type switching and recombination repair in fission yeast. *Proc Natl Acad Sci USA* **100**: 15770–15775
- Allers T, Lichten M (2001) Differential timing and control of non-crossover and crossover recombination during meiosis. *Cell* **106**: 47–57
- Arcangioli B, de Lahondes R (2000) Fission yeast switches mating type by a replication–recombination coupled process. *EMBO J* **19**: 1389–1396
- Arcangioli B, Thon G (2004) Mating-type cassettes: structure, switching and silencing. In *The Molecular Biology of Schizosaccharomyces pombe*, Egal R (ed) pp 129–148. Heidelberg: Springer
- Bishop DK, Park D, Xu L, Kleckner N (1992) *DMC1*: a meiosis-specific yeast homolog of *E. coli recA* required for recombination, synaptonemal complex formation, and cell cycle progression. *Cell* **69**: 439–456
- Börner GV, Kleckner N, Hunter N (2004) Crossover/noncrossover differentiation, synaptonemal complex formation, and regulatory surveillance at the leptotene/zygotene transition of meiosis. *Cell* **117**: 29–45
- Brenneman MA, Wagener BM, Miller CA, Allen C, Nickoloff JA (2002) XRCC3 controls the fidelity of homologous recombination: roles for XRCC3 in late stages of recombination. *Mol Cell* **10**: 387–395
- Caspari T, Murray JM, Carr AM (2002) Cdc2-cyclin B kinase activity links Crb2 and Rqh1-topoisomerase III. *Genes Dev* **16**: 1195–1208
- Dalgaard JZ, Klar AJ (2001) A DNA replication-arrest site RTS1 regulates imprinting by determining the direction of replication at *mat1* in *S. pombe*. *Genes Dev* **15**: 2060–2068
- Doe CL, Osman F, Dixon J, Whitby MC (2004) DNA repair by a Rad22–Mus81-dependent pathway that is independent of Rhp51. *Nucleic Acids Res* **32**: 5570–5581
- Egel R, Beach DH, Klar AJ (1984) Genes required for initiation and resolution steps of mating-type switching in fission yeast. *Proc Natl Acad Sci USA* **81**: 3481–3485
- Ekwall K, Javerzat JP, Lorentz A, Schmidt H, Cranston G, Allshire R (1995) The chromodomain protein *Swi6*: a key component at fission yeast centromeres. *Science* **269**: 1429–1431
- Ellermeier C, Schmidt H, Smith GR (2004) *Swi5* acts in meiotic DNA joint molecule formation in *Schizosaccharomyces pombe*. *Genetics* **168**: 1891–1898
- Hagan IM, Hyams JS (1988) The use of cell division cycle mutants to investigate the control of microtubule distribution in the fission yeast *Schizosaccharomyces pombe*. *J Cell Sci* **89**: 343–357
- Haruta N, Kurokawa Y, Murayama Y, Akamatsu Y, Unzai S, Tsutsui Y, Iwasaki H (2006) The *Swi5*–*Sfr1* complex stimulates Rhp51/Rad51- and Dmcl1-mediated DNA strand exchange *in vitro*. *Nat Struct Mol Biol* **13**: 823–830
- Hayase A, Takagi M, Miyazaki T, Oshiumi H, Shinohara M, Shinohara A (2004) A protein complex containing Mei5 and Sae3 promotes the assembly of the meiosis-specific RecA homolog Dmcl1. *Cell* **119**: 927–940
- Hunter N, Kleckner N (2001) The single-end invasion: an asymmetric intermediate at the double-strand break to double-Holliday junction transition of meiotic recombination. *Cell* **106**: 59–70
- Ira G, Malkova A, Liberi G, Foiani M, Haber JE (2003) Srs2 and Sgs1–Top3 suppress crossovers during double-strand break repair in yeast. *Cell* **115**: 401–411
- Jia S, Yamada T, Grewal SI (2004) Heterochromatin regulates cell type-specific long-range chromatin interactions essential for directed recombination. *Cell* **119**: 469–480
- Khasanov FK, Savchenko GV, Bashkirova EV, Korolev VG, Heyer WD, Bashkirov VI (1999) A new recombinational DNA repair gene from *Schizosaccharomyces pombe* with homology to *Escherichia coli* RecA. *Genetics* **152**: 1557–1572
- Klar AJ (1992) Developmental choices in mating-type interconversion in fission yeast. *Trends Genet* **8**: 208–213
- Krogh BO, Symington LS (2004) Recombination proteins in yeast. *Annu Rev Genet* **38**: 233–271
- Liu Y, Masson JY, Shah R, O’Regan P, West SC (2004) RAD51C is required for Holliday junction processing in mammalian cells. *Science* **303**: 243–246
- McKee AH, Kleckner N (1997) Mutations in *Saccharomyces cerevisiae* that block meiotic prophase chromosome metabolism and confer cell cycle arrest at pachytene identify two new meiosis-specific genes *SAE1* and *SAE3*. *Genetics* **146**: 817–834
- Miyazaki T, Bressan DA, Shinohara M, Haber JE, Shinohara A (2004) *In vivo* assembly and disassembly of Rad51 and Rad52 complexes during double-strand break repair. *EMBO J* **23**: 939–949
- Moreno S, Klar A, Nurse P (1991) Molecular genetic analysis of fission yeast *Schizosaccharomyces pombe*. *Methods Enzymol* **194**: 795–823
- Muris DF, Vreeken K, Carr AM, Broughton BC, Lehmann AR, Lohman PH, Pastink A (1993) Cloning the *RAD51* homologue of *Schizosaccharomyces pombe*. *Nucleic Acids Res* **21**: 4586–4591
- Muris DF, Vreeken K, Carr AM, Murray JM, Smit C, Lohman PH, Pastink A (1996) Isolation of the *Schizosaccharomyces pombe* *RAD54* homologue, *rhp54*⁺, a gene involved in the repair of radiation damage and replication fidelity. *J Cell Sci* **109**: 73–81
- Muris DF, Vreeken K, Schmidt H, Ostermann K, Clever B, Lohman PH, Pastink A (1997) Homologous recombination in the fission yeast *Schizosaccharomyces pombe*: different requirements for the *rhp51*⁺, *rhp54*⁺ and *rad22*⁺ genes. *Curr Genet* **31**: 248–254

- Ostermann K, Lorentz A, Schmidt H (1993) The fission yeast *rad22* gene, having a function in mating-type switching and repair of DNA damages, encodes a protein homolog to Rad52 of *Saccharomyces cerevisiae*. *Nucleic Acids Res* **21**: 5940–5944
- Paques F, Haber JE (1999) Multiple pathways of recombination induced by double-strand breaks in *Saccharomyces cerevisiae*. *Microbiol Mol Biol Rev* **63**: 349–404
- Prudden J, Evans JS, Hussey SP, Deans B, O'Neill P, Thacker J, Humphrey T (2003) Pathway utilization in response to a site-specific DNA double-strand break in fission yeast. *EMBO J* **22**: 1419–1430
- Sugawara N, Wang X, Haber JE (2003) *In vivo* roles of Rad52, Rad54, and Rad55 proteins in Rad51-mediated recombination. *Mol Cell* **12**: 209–219
- Sung P (1997) Yeast Rad55 and Rad57 proteins form a heterodimer that functions with replication protein A to promote DNA strand exchange by Rad51 recombinase. *Genes Dev* **11**: 1111–1121
- Symington LS (2002) Role of *RAD52* epistasis group genes in homologous recombination and double-strand break repair. *Microbiol Mol Biol Rev* **66**: 630–670
- Szostak JW, Orr-Weaver TL, Rothstein RJ, Stahl FW (1983) The double-strand-break repair model for recombination. *Cell* **33**: 25–35
- Tsubouchi H, Roeder GS (2004) The budding yeast Mei5 and Sae3 proteins act together with dmc1 during meiotic recombination. *Genetics* **168**: 1219–1230
- Tsutsui Y, Morishita T, Iwasaki H, Toh H, Shinagawa H (2000) A recombination repair gene of *Schizosaccharomyces pombe*, *rhp57*, is a functional homolog of the *Saccharomyces cerevisiae* *RAD57* gene and is phylogenetically related to the human *XRCC3* gene. *Genetics* **154**: 1451–1461
- Wu L, Hickson ID (2003) The Bloom's syndrome helicase suppresses crossing over during homologous recombination. *Nature* **426**: 870–874